noff-Lehrman, S., Blum, R. M., Barry, D. W., Shearer, G. M., Fischl, M. A., Mitsuya, H., Gallo, R. C., Collins, J. M., Bolognesi, D. P., Myers, C. E., & Broder, S. (1986) *Lancet i*, 575–580.

Yarchoan, R., Mitsuya, H., Myers, C. E., & Broder, S. (1989) *New Engl. J. Med. 321*, 726–738.

Yoshikawa, M., Kata, T., & Takenishi, T. (1967) *Tetrahedron Lett.*, 5065–5084.

Articles

Kinetic Mechanism of DNA Polymerase I (Klenow Fragment): Identification of a Second Conformational Change and Evaluation of the Internal Equilibrium Constant†,‡

Michael E. Dahlberg and Stephen J. Benkovic*

Department of Chemistry, The Pennsylvania State University, University Park, Pennsylvania 16802

Received August 20, 1990; Revised Manuscript Received February 8, 1991

ABSTRACT: In a previously determined minimal kinetic scheme for DNA polymerization catalyzed by the Klenow fragment (KF) of *Escherichia coli* DNA polymerase I, a nonchemical step that interconverted the KF′·DNA$_{n+1}$·PP$_i$ and KF·DNA$_{n+1}$·PP$_i$ complexes was not observed in correct incorporation [Kuchta, R. D., Mizrahi, V., Benkovic, P. A., Johnson, K. A., & Benkovic, S. J. (1987) *Biochemistry 26*, 8410–8417] but was detected in misincorporation [Kuchta, R. D., Benkovic, P. A., & Benkovic, S. J. (1988) *Biochemistry 27*, 6716–6725]. In a pulse–chase experiment in this study, a burst amplitude of 100% of the enzyme concentration is observed; under pulse–quench conditions, the burst amplitude is 80%, indicative of the accumulation of the KF′·DNA·dNTP species owing to a slow step subsequent to chemical bond formation. This latter step was unequivocally identified by single-turnover pyrophosphorolysis and pyrophosphate-exchange experiments as one interconverting KF′·DNA$_{n+1}$·PP$_i$ and KF·DNA$_{n+1}$·PP$_i$. The rate constants for this step in both directions were established through the rate constants for processive synthesis and pyrophosphorolysis. Pyrophosphorolysis of a 3′-phosphorothioate DNA duplex confirmed that the large elemental effect observed previously [Mizrahi, V., Henrie, R. N., Marlier, J. F., Johnson, K. A., & Benkovic, S. J. (1985) *Biochemistry 24*, 4010–4018] in this direction but not in polymerization is due to a marked decrease in the affinity of KF for the phosphorothioate-substituted duplex and not to the chemical step. The combination of the experimentally measured equilibrium constant for the bound KF·DNA species with the collective kinetic measurements further extends previous insights into the dynamics of the polymerization process catalyzed by KF.

The Klenow fragment (KF)[1] of *Escherichia coli* DNA polymerase I contains two domains that reside on a single polypeptide chain. Unlike pol I, which has a 5′ → 3′ and a 3′ → 5′ exonuclease as well as a polymerase activity, KF has been shown to exhibit only the 3′ → 5′ exonuclease and polymerase activities (Kornberg, 1980). The polymerase activity, which resides on the larger of the two domains, has been the object of intense investigation including stereochemical (Burgers & Eckstein, 1979; Brody & Frey, 1981; Gupta & Benkovic, 1984), structural (Ollis et al., 1985; Freemont et al., 1988), and kinetic analyses (McClure & Jovin, 1975; Bambara et al., 1976; Bryant et al., 1983; Mizrahi et al., 1985, 1986a; Kuchta et al., 1987, 1988). The previously proposed kinetic pathway by which a nucleotide is correctly incorporated (Kuchta et al., 1987) involves the ordered binding of DNA then dNTP followed by a slow nonchemical event that limits the rate for a single incorporation event. Phosphodiester bond formation then occurs, which is followed by PP$_i$ release. KF then partitions between additional nucleotide incorporation or dissociation from the DNA.[2]

KF presents an ideal model (Carroll & Benkovic, 1990) with which to study the low error frequency in the synthesis of DNA owing to its relatively slow rate of polymerization compared to the bacteriophage polymerases, small size (approximately 68 000 daltons), and lack of accessory proteins. The fidelity with which pol I replicates a template strand has been estimated to be as low as 10^{-8} to 10^{-12} errors per nucleotide incorporated (Englisch et al., 1985). Recently, the kinetic mechanism for incorrect nucleotide addition to a duplex by KF has been elucidated (Kuchta et al., 1988). The mechanism

† This work was supported by NIH Grant GM13306.

‡ In honor of Dr. Robert Abeles on the occasion of his 65th birthday. We wish him many more.

* Author to whom correspondence should be addressed.

[1] Abbreviations: Pol I, *E. coli* DNA polymerase I; KF, Klenow fragment of pol I; KF(exo$^-$), (Asp355Ala, Glu357Ala) KF mutant devoid of any exonuclease activity; dNTP, deoxynucleoside 5′-triphosphate; PP$_i$, inorganic pyrophosphate; TEAB, triethylammonium bicarbonate; Tris·HCl, tris(hydroxymethyl)aminomethane hydrochloride salt; EDTA, ethylenediaminetetraacetate sodium salt.

[2] It is gratifying to note that the principal kinetic features originally described for the polymerization of DNA catalyzed by KF also apply to T7 DNA polymerase (Patel et al., 1991).

0006-2960/91/0430-4835$02.50/0

postulates that KF goes through three stages of nucleotide discrimination: the first, where the greatest differentiation occurs, includes the nucleotide binding and chemical catalysis steps; the second is comprised of a conformational change step that occurs after catalysis but prior to PP_i release and increases the reaction time for exonucleolytic editing; the third encompasses the partitioning of the mismatched primer terminus between addition of a correct nucleotide and its exonucleolytic removal.

While the conformational change step identified in the second stage had been fully characterized under misincorporation conditions, there was no evidence to suggest that this step was important in the pathway for correct incorporation. In this report we describe evidence for the occurrence of this step through combination of pre-steady-state pyrophosphorolysis and pyrophosphate-exchange measurements and pulse–chase experiments, which serve to locate this step and to identify the ternary intermediates separated by it. The measurements of the rate constants for processive synthesis and of an equilibrium constant for the enzyme–DNA-bound species permit the magnitude of this conformational change step to be evaluated. These findings, coupled with the previous minimal kinetic scheme for KF (Kuchta et al., 1987), permit a more complete description of the free energy requirements for correct nucleotide incorporation at the primer terminus of a duplex by KF.

Experimental Procedures

Materials. KF was purified from *E. coli* CJ155 according to established procedures (Joyce & Grindley, 1983). The KF(exo$^-$) mutant was purified as described previously (Eger et al., 1991). Both *E. coli* strains were provided by Professor C. Joyce. The concentration of KF was determined spectrophotometrically, by use of $\epsilon_{278} = 6.32 \times 10^4\ M^{-1}\ cm^{-1}$ (Setlow et al., 1972), and by burst amplitude measurements in the presence of a saturating concentration of DNA. In the latter method, the amplitude of the fast phase is indicative of the active enzyme concentration and agrees well with the spectroscopic method. T4 polynucleotide kinase was from U.S. Biochemical Corp. Acetyl-CoA synthetase and yeast inorganic pyrophosphatase were from Sigma.

Radionucleotides [γ-^{32}P]ATP, [α-^{32}P]dATP, [α-^{35}S]-dATP(αS), and [α-^{32}P]TTP were from New England Nuclear. All unlabeled dNTP's of the highest possible purity were obtained from Pharmacia. Na_4PP_i, obtained from Sigma, was purified according to a published procedure (Kuchta et al., 1987). PP_i purity and concentrations were determined by use of ^{31}P NMR, comparing a sample to a known amount of K_3PO_4. Confirmation was obtained through the use of the colorimetric assay of Lanzetta et al. (1979) following treatment of the samples with pyrophosphatase. Coenzyme A (CoA) was obtained from Sigma as were all Sephadex resins and buffer components.

Preparation of DNA Duplexes. Oligonucleotides were synthesized on an Applied Biosystems 380A DNA synthesizer and purified by gel electrophoresis. Oligonucleotide duplexes were formed by mixing equimolar amounts of template and primer strands in 50 mM Tris·HCl, pH 7.5. This solution was brought to 75 °C, maintained at this temperature for 10 min, and then allowed to cool to room temperature over the course of 2–3 h. The DNA duplexes used in these experiments are shown in Chart I.

DNA duplex concentrations of the 13/20mer were determined by measuring incorporation of [^{32}P]dAMP under conditions similar to those described under the 3′-^{32}P-end-labeling protocol.

Chart I

```
                (5')                (3')
9/20 mer          TCGCAGCCG
                  AGCGTCGGCAGGTTCCCAAA

                (5')                    (3')
13/20 mer         TCGCAGCCGTCCA
                  AGCGTCGGCAGGTTCCCAAA
```

5′-^{32}P-End Labeling of Duplex. The 5′-^{32}P-end labeling of DNA was performed as described previously (Mizrahi et al., 1986b).

3′-^{32}P-End Labeling of Duplex. The [3′-^{32}P]14/20mer substrate was prepared by incubating 2.0 μM 13/20mer, 5.0 μM KF(exo$^+$), 10 μM [α-^{32}P]dATP ($\sim 6 \times 10^5$ cpm pmol^{-1}), 5 mM $MgCl_2$, and 50 mM Tris·HCl, pH 7.5, for 10 s in a total volume of 50 μL. The reaction was stopped by the addition of 50 μL of 0.1 M EDTA followed by phenol–chloroform extraction of the enzyme according to established techniques (Maniatis et al., 1982). The reaction product was purified by passage through two spun columns, the preparation of which is described in Maniatis et al. (1982). To determine that all the primer had been extended and that no significant misincorporation had taken place, a sample was 5′-^{32}P-end-labeled and analyzed by gel electrophoresis. The results showed that all the 13/20mer had been extended to 14/20mer and that no 14A/20mer (the misincorporation product of 14/20mer and dATP) was present. To ascertain that all remaining [α-^{32}P]dATP had been removed by the spun columns, a sample of the reaction mixture was analyzed by TLC. Typically, less than 1.5% of the total radioactivity present existed as [α-^{32}P]dATP. The [3′-^{35}S]14/20mer substrate was prepared similarly except [α-^{32}P]dATP was replaced with [α-^{35}S]dATP(αS) ($\sim 1.1 \times 10^6$ dpm pmol^{-1}), 1 mM dithiothreitol (DTT) was included, and the reaction was allowed to incubate for 60 s.

Preparation of [^{32}P]PP_i. For use in the pyrophosphate-exchange experiments, it was necessary to prepare [^{32}P]PP_i in high specific activity. In a total volume of 50 μL, 15 μM CoA, 15 μM potassium acetate, 5 units of acetyl-CoA synthetase, 2.3 μM [γ-^{32}P]ATP (3000 Ci mmol^{-1}), 1 mM DTT, 10 mM $MgCl_2$, and 50 mM Tris·HCl, pH 7.5, were incubated for 30 min at 37 °C. The reaction was quenched by heating the solution to 75 °C for 10 min and then placing it on ice. The [^{32}P]PP_i was purified by TLC. Areas of the TLC containing the PP_i were soaked in 1 M TEAB, pH 7.6, overnight. The solution was then diluted 1:10 and loaded on a DEAE-Sephadex A-25 column preequilibrated at 0.3 M TEAB. The column was washed with 0.4 M TEAB, and the [^{32}P]PP_i was eluted with 0.5 M TEAB. The eluent was vacuum-dried and was taken up in 50 mM Tris·HCl, pH 7.5. The purity was tested by subjecting a sample to pyrophosphatase degradation and then analyzing the mixture by TLC. It was observed that all radioactivity was converted to a form that migrated with P_i, indicating that any unreacted [γ-^{32}P]ATP was removed during the purification process.

DNA Filter Binding Assays. Radioactivity present in DNA was determined according to a previously described procedure (Bryant et al., 1983). Filters were mixed with Fisher Scintiverse II and counted in a Beckman LS8100 or LS6800 scintillation counter.

Gel Electrophoresis. Denaturing polyacrylamide gel electrophoresis and autoradiography were performed as described previously (Mizrahi et al., 1986b). All gels contained 20% acrylamide.

TLC Analysis. Samples labeled with [α-^{32}P]dATP were spotted on Whatman poly(ethylenimine)–cellulose plates with a fluorescent indicator and eluted with 0.3 M potassium phosphate, pH 8.0. Those labeled with [α-^{35}S]dATP(αS) were eluted with a buffer containing 0.5 M K_2HPO_4 and 0.01 M β-mercaptoethanol. The TLC plate was then exposed to Kodak XAR film for a variable length of time. The entire TLC plate was cut into sections and counted. The radioactivity in the section of interest was normalized to the total amount of radioactivity on the plate.

Quench Control Experiments. The effectiveness of a quench solution on the pre-steady-state kinetics of polymerization was determined by mixing equal volumes (30 μL) of KF·9/20mer and Mg·[α-^{32}P]TTP solutions in the rapid-quench apparatus, the design of which has been described previously (Johnson, 1986). The KF·9/20mer solution contained 120 nM KF(exo$^-$), 400 nM 9/20mer, and 2.5 mM EDTA in 50 mM Tris·HCl, pH 7.5. The Mg·[α-^{32}P]TTP solution contained 10 μM TTP ($\sim$10 000 cpm pmol^{-1}) and 12.5 mM $MgCl_2$ in 50 mM Tris·HCl, pH 7.5. The reaction was held at a constant temperature of 22 °C. At time points between 4 ms and 1 s, the reaction was quenched with 184 μL of HCl (final concentration 0.037–0.8 N), NaOH (final concentration 0.5–1.5 M) or EDTA (final concentration 0.075 M). If an acid quench was used, the solution was collected in a tube containing 100 μL of $CHCl_3$, vortexed, and neutralized with 3 N KOH dissolved in 1 M Tris within 30 s to avoid decomposition of products. Under these conditions, dATP, PP_i, 13mer, and 14mer are stable as judged by either TLC or gel electrophoresis. The amount of radioactivity incorporated into the 9/20mer was determined by the filter binding assay.

Pulse–Chase Experiments. The pulse–chase experiments were also done with the rapid-quench apparatus. The KF·DNA solution contained 800 nM 13/20mer, 250 nM KF(exo$^+$), and 2.5 mM EDTA in 50 mM Tris·HCl, pH 7.5. The Mg·[α-^{32}P]dATP solution contained 10 μM dATP ($\sim$10 000 cpm pmol^{-1}) and 12.5 mM $MgCl_2$ in 50 mM Tris·HCl, pH 7.5. After 4 ms to 1 s, the reaction was either quenched with 184 μL of 1.09 N HCl (final concentration 0.8 N) or chased with 6.8 mM dATP (final concentration 5 mM). If the reaction was quenched with acid, then 64.8 μL of H_2O was added to the tube and it was processed as described in the previous experiment. If the reaction was chased with dATP, then it was collected in a tube containing 64.8 μL of 3.1 N HCl (final concentration 0.8 N) and 100 μL of $CHCl_3$ and then vortexed. The solution was then neutralized with 3 N KOH dissolved in 1 M Tris. The amount of radioactivity incorporated into the 13/20mer was determined by the filter binding assay.

Single-Turnover Pyrophosphorolysis Experiments. By use of the rapid-quench apparatus, the reaction was initiated by mixing a KF·[^{32}P]14/20mer solution with a Mg·dATP·PP_i solution. The KF·[^{32}P]14/20mer solution contained 70 nM 3′-^{32}P-end-labeled 14/20mer, 700 nM KF(exo$^+$), and 2.5 mM EDTA in 50 mM Tris·HCl, pH 7.5. The Mg·dATP·PP_i solution contained 10 μM dATP, 0.07–2.0 mM PP_i, and $MgCl_2$ at a concentration 12.5 mM above twice the PP_i concentration in 50 mM Tris·HCl, pH 7.5. At time points between 747 ms and 16 s, the reaction was quenched with HCl to a final concentration of 0.8 N and processed as described above. The amounts of [α-^{32}P]dATP formed via pyrophosphorolysis and [^{32}P]dAMP produced by the exonuclease were quantitated by TLC.

Elemental Effects on DNA Binding. The reaction to determine the dissociation constant of [3′-^{32}P]14/20mer was initiated by mixing an equal volume (40 μL) of a solution containing 20 μM dATP, 2 mM PP_i, 650 μg/mL calf thymus DNA, and 12.5 mM $MgCl_2$ in 50 mM Tris·HCl, pH 7.5, with a solution containing 25 nM KF(exo$^+$), 14–70 nM [3′-^{32}P]-14/20mer, and 2.5 mM EDTA in 50 mM Tris·HCl, pH 7.5. Aliquots were taken at time points between 0 and 60 s, quenched in 0.1 M EDTA, and processed by TLC as described above. Identical reactions were done to ascertain the dissociation constant for ^{35}S-labeled 14/20mer except the DNA in the second solution was replaced with 200–1000 nM [3′-^{35}S]14/20mer, 2.5 mM DTT was added to the second solution, and time points were taken between 0 and 120 s.

Pyrophosphate-Exchange Experiments. The pyrophosphate-exchange experiments were conducted by mixing 500 nM 13/20mer, 1.0 μM KF(exo$^+$), 20 μM dATP, 35–140 μM PP_i ($\sim$500 cpm pmol^{-1}), and 5 mM $MgCl_2$ in 50 mM Tris·HCl, pH 7.5, in a total volume of 100 μL. Time points were taken between 0 and 90 s. For each time point, a 5-μL aliquot was taken and quenched into 5 μL of 0.1 M EDTA. The amount of [^{32}P]PP_i converted to [^{32}P]dATP was then determined by TLC analysis.

Processive Synthesis Measurements. By use of the rapid quench apparatus, the rate of elongation of the 13/20mer to the 17/20mer was measured. The KF·13/20mer solution contained 200 nM 5′-^{32}P-end-labeled 13/20mer, 800 nM KF(exo$^+$), and 2.5 mM EDTA in 50 mM Tris·HCl, pH 7.5. The Mg·dNTP solution contained 20 μM dATP, 60 μM dGTP, and 12.5 mM $MgCl_2$ in 50 mM Tris·HCl, pH 7.5. Time points were taken between 4 ms and 1 s. The reaction was quenched with acid to a final concentration of 0.8 N HCl and processed as described above. The amounts of 13mer, 14mer, 15mer, 16mer, and 17mer formed were determined by gel electrophoresis and autoradiography.

As a control experiment to assess the effect of sequence on processive synthesis, 5′-^{32}P-end-labeled 14/20mer was prepared and then used in a similar set of reaction conditions as described above. The 5′-^{32}P-end-labeled 13/20mer was elongated to the end-labeled 14/20mer under reaction conditions identical with the 3′-^{32}P-end-labeling reaction conditions described above except unlabeled dATP was used in place of [α-^{32}P]-dATP. The 5′-^{32}P-end-labeled 14/20mer was then purified, quantitated, and tested for purity as described in the 3′-^{32}P-end-labeling section. It was then used in the KF·14/20mer solution, which contained 50 nM 5′-^{32}P-end-labeled 14/20mer, 200 nM KF(exo$^+$), and 2.5 mM EDTA in 50 mM Tris·HCl, pH 7.5. The Mg·dNTP solution was identical with the one in the previously described processive synthesis experiment, as were the time points taken, the reaction quench, and the reaction work-up.

Equilibrium Measurements. The overall equilibrium constant for bound DNA for the polymerization reaction catalyzed by KF was measured by use of the rapid-quench apparatus. The KF·13/20mer solution contained 200 nM 5′-^{32}P-end-labeled 13/20mer, 500 nM KF(exo$^+$), and 2.5 mM EDTA in 50 mM Tris·HCl, pH 7.5. The Mg·dATP·PP_i solution contained 800 nM dATP, 0–2 mM PP_i, and 12.5 mM $MgCl_2$ in 50 mM Tris·HCl, pH 7.5. Time points were taken between 0 and 9 s. The reaction was quenched with acid to a final HCl concentration of 0.8 N. The amounts of 13mer and 14mer were quantitated by gel electrophoresis and autoradiography.

Computer Simulations. Computer simulations of the time courses obtained in each experiment were done with a modification (Anderson et al., 1988) of the kinetic simulation program KINSIM (Barshop et al., 1983). The data were initially fit to the individual schemes shown in the Results and Dis-

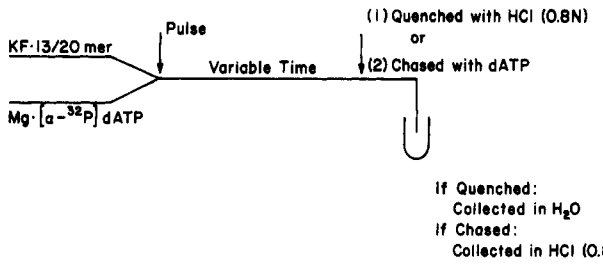

FIGURE 1: Pictorial representation of the pulse–chase experiments described in the text.

cussion sections; however, all time courses were eventually shown to obey the complete kinetic mechanism described in Scheme V. Some data were fit with the program RSI (BBN Software Products Corp.).

RESULTS

Quench Comparison Studies. The efficiency of an EDTA quench was evaluated by comparing a single incorporation of dATP into a 5′-end-labeled 13/20mer by KF by use of either EDTA, acid, or base to quench the reaction. With NaOH at a final quench concentration of 0.5–1.5 M, results were obtained indicative of poor quenching, since total incorporation was observed at all time points. Final HCl concentrations of 0.45–0.8 M gave coincident biphasic curves, while lower concentrations of acid resulted in a significant scatter of the data owing to incomplete quenching. Direct comparison of a single incorporation assay with use of EDTA at a final concentration of 0.075 M and HCl at a final concentration of 0.8 M provided identical initial pre-steady-state and steady-state rates regardless of the nature of the quench. They differed, however, in the burst amplitudes (data not shown). When EDTA was used as a quench, a burst amplitude equal to 1 enzyme equiv was obtained, in contrast to an 0.8 enzyme equiv burst amplitude when HCl was used as quench. Although KF(exo$^-$) was used in this set of experiments, Eger et al. have shown that its kinetic properties for the polymerase activity are equivalent to wild type (Eger et al., 1991). On the basis of this result, all the following experiments using single-turnover conditions were done with an acid quench.

Pulse–Chase Experiments. On the basis of the difference between the acid and EDTA quench results, experiments were done to assess the partitioning of the ternary complexes along the polymerase pathway. As shown in Figure 1, an experiment was conducted by mixing KF·13/20mer with Mg·[α-^{32}P]-dATP; the solution was allowed to react for a variable length of time, and then the reaction was either quenched with acid or chased with a 1000-fold excess of unlabeled dATP. If the reaction was chased, then it was ultimately quenched with acid approximately 50 ms later. The results are shown in Figure 2. The initial rates were identical in each experiment as were the slower steady-state rates. However, as was observed in the experiments to test the quench efficiency, the burst amplitude was 80% of the active enzyme concentration under pulse–quench conditions. Under pulse–chase conditions, the burst amplitude was equivalent to 100% of the active enzyme concentration.

Pyrophosphorolysis. Single-turnover pyrophosphorolysis rates were measured according to the reaction in Scheme I. With use of rapid quench techniques, the experiment was initiated by mixing a solution of KF, in 10-fold excess of DNA, and 3′-end-labeled 14/20mer with a solution of dATP and PP_i; the resulting solution was allowed to react for a variable length of time and then quenched with acid. The production of radiolabeled dATP was monitored by TLC. The time course

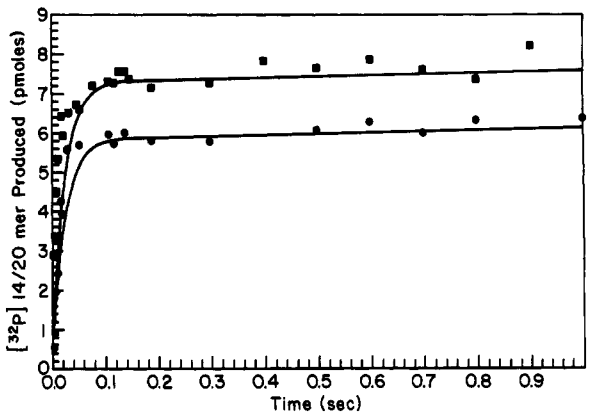

FIGURE 2: Pulse–chase experimental results. The incorporation of radiolabeled dATP into the 13/20mer was measured under either pulse–chase (■) or pulse–quench (●) conditions. The simulated curves were modeled to the kinetic mechanism described in Scheme V and the rate and equilibrium constants in Table II. On the basis of the values presented under Experimental Procedures, there are 7.5 pmol of active KF in each time point. The curve representative of the pulse–quench data predicts the rate of formation of all DNA_{n+1} species; the simulated curve for the pulse–chase data predicts the rate of formation for all DNA_{n+1} and adds the KF′·DNA·dNTP species.

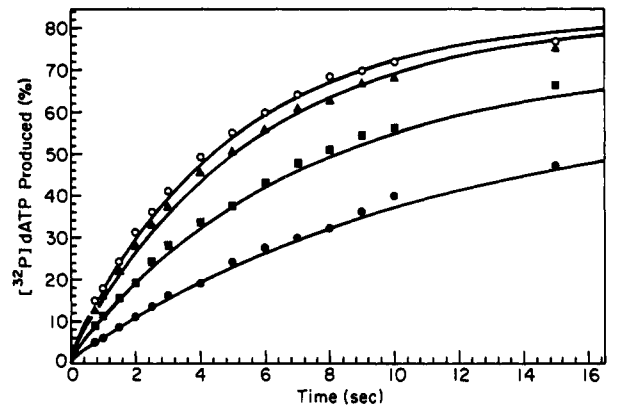

FIGURE 3: Single-turnover pyrophosphorolysis. The rate of formation of radiolabeled dATP from 3′-end-labeled 14/20mer and 100 (●), 250 (■), 500 (▲), or 1000 μM (○) PP_i was measured. The curves are computer fits of the data to the kinetic mechanism in Scheme V and the rate and equilibrium constants in Table II.

of the reaction in response to varying levels of PP_i is shown in Figure 3. The observed rate constants for each reaction were determined by a computer fit of the data to a single-exponential equation. A secondary plot fitting these rate constants at their respective substrate concentrations to the Michaelis–Menten equation (data not shown) gave an apparent pyrophosphorolysis rate constant (k_{pyro}) of 0.31 s^{-1} and a Michaelis constant (K_M) of 230 μM. Since this reaction was constrained to a single-turnover event, and given the relative magnitude of K_M to k_{pyro}, the observed Michaelis constant probably represents a true dissociation constant.

Scheme I

$$E\cdot[3'\text{-}^{32}P]14/20mer + PP_i \overset{K_D}{\rightleftharpoons} E\cdot[3'\text{-}^{32}P]14/20mer\cdot PP_i \xrightarrow{k_{pyro}} E\cdot 13/20mer + [\alpha\text{-}^{32}P]dATP$$

Several reaction conditions were selected to ensure that only a single turnover of the enzyme was observed. Given a K_D for the 13/20mer of 5 nM and a concentration of enzyme to DNA of 10:1, all of the duplex oligomer will be enzyme-bound. Further, by use of TLC to analyze the time points of the

reaction directly for dATP, the loss of label from the 14/20mer due to KF's associated exonuclease activity can be ignored. Finally, the presence of a pool of unlabeled dATP serves, by dilution, to prevent the return of labeled product to labeled substrate.

The effect of various concentrations of unlabeled dATP on the pyrophosphorolysis reaction was examined (data not shown). The results indicate that there is little change in the rate of the reaction at dATP concentrations between 1 and 20 μM, and therefore, the competitive effects of this pool of unlabeled product on the binding of PP_i to the E·DNA complex are negligible. However, without a means of trapping the labeled dATP that is produced ([dATP] = 0 μM), the reaction rapidly approaches an equilibrium level of 20% turnover of the E·DNA complex.

Elemental Effects on DNA Binding. The dissociation constants of the [3′-^{35}S]14/20mer and the [3′-^{32}P]14/20mer to KF were determined by quantitating the extent of pyrophosphorolysis at saturating PP_i and varying DNA concentrations. Unlabeled dATP was used to trap product as described in the pyrophosphorolysis experiments; calf thymus DNA was used to trap any unbound 14/20mer. The concentration of [^{32}P]dATP formed at 0 s was determined at a given 14/20mer concentration by extrapolation, plotted versus initial 14/20mer concentration, and fit to the quadratic form of the binding equation. The dissociation constant determined for the [3′-^{35}S]14/20mer is 184 ± 5 nM, while for the [3′-^{32}P]14/20mer it is 5.3 ± 0.9 nM. This represents an elemental effect of 36 on DNA binding.

Pyrophosphate Exchange. As shown in Scheme II, the pyrophosphate-exchange experiments were designed to measure the exchange of a radiolabel from pyrophosphate to dATP under polymerization conditions. The reaction was initiated by addition of KF to a solution of the 13/20mer, dATP, and varying levels of [^{32}P]PP_i, the solution was quenched with EDTA, and the products were separated on TLC. From measurements of the rate of pyrophosphate exchange at PP_i concentrations of 35 and 140 μM, the rate constant for pyrophosphate exchange at a saturating PP_i concentration was calculated to be 0.17 ± 0.07 s^{-1}.

Scheme II

$$dATP + [^{32}P]PP_i \underset{}{\overset{KF\cdot 13/20mer}{\rightleftharpoons}} [^{32}P]dATP + PP_i$$

Processivity Measurements. The rate of incorporation of successive nucleotides into the 13/20mer was determined in this experiment. KF was incubated with 5′-end-labeled 13/20mer in the quench–flow apparatus and mixed with a solution of dATP and dGTP to form ultimately a 17/20mer duplex. Time points were processed by gel electrophoresis and radioactivity representing 13mer, 14mer, 15mer, 16mer, and 17mer was excised and counted. The time course is shown in Figure 4. The best fit of the resulting data points was obtained when Scheme III was used as a model. The data show that while the first incorporation of dATP occurs at a rate commensurate with the rate of the first conformational change (approximately 50 s^{-1}), addition of successive nucleotides is slowed considerably. In fact, the addition of dGTP to the newly formed 14/20mer duplex could not be fit without addition of a slow, second nonchemical step that occurred with a rate constant of approximately 15 s^{-1}.

To determine whether this was a real phenomenon or merely a sequence-dependent artifact, the 5′-end-labeled 14/20mer was made and used in the above experiment in place of the 5′-end-labeled 13/20mer. Further, dATP was included in the reaction to test for inhibitory effects of an incorrect nucleotide.

Scheme III

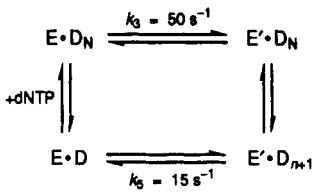

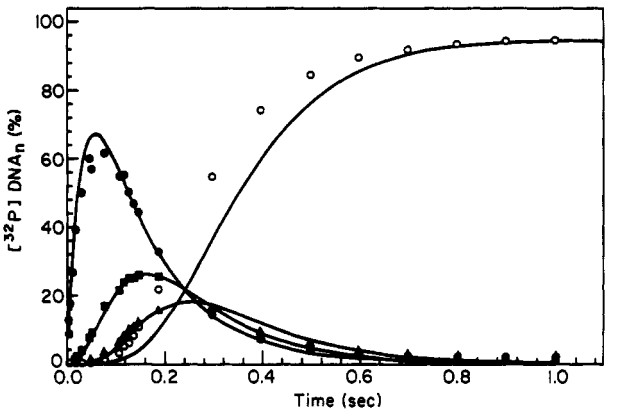

FIGURE 4: Processive synthesis experiments. The rate of elongation of 5′-end-labeled 13/20mer to form 14/20mer (●), 15/20mer (■), 16/20mer (▲), and 17/20mer (○) was measured as described under Experimental Procedures. The data was fit to the mechanism described in Scheme III. The values for the dNTP dissociation constant, k_3, and k_5 are in Table II. (A forward rate constant of 4000 s^{-1} and a reverse rate constant of 1000 s^{-1} were used for the conversion of E′·D_N to E′·D_{n+1} in order to maintain this reaction segment of Scheme III at equilibrium.)

Table I: Measurements of the Equilibrium between KF·13/20mer and KF·14/20mer[a]

$[PP_i]$ (μM)	14/20mer (%)[b]	K_{EQ}[c]
250	90.4 ± 2.1	3478
500	86.4 ± 2.3	3082
1000	74.8 ± 0.6	1726
av K_{EQ}		2762 ± 919

[a] Obtained as described under Experimental Procedures. [b] Control experiments indicated that 25% of the 5′-end-labeled 13mer existed as single-stranded DNA rather than in a 13/20mer duplex, and therefore, it is not catalytically active. The values presented here are corrected for this contaminant. [c] Calculated from the following equation K_{EQ} = ([PP_i][KF·14/20mer])/([dATP]$_F$[KF·13/20mer]$_F$) where [KF·14/20mer] = [14/20mer]$_{ex}$ − [KF·14/20mer·PP_i] and [KF·14/20mer·PP_i] = ([PP_i][KF·14/20mer])/K_D^{PPi}. Therefore, [KF·14/20mer] = [14/20mer]$_{ex}$/(1 + [PP_i]/K_D^{PPi}) where [14/20mer]$_{ex}$ is the experimentally determined 14/20mer concentration and subscript F refers to the final calculated concentration of these species. Since this experiment measures the 14/20mer, whether free or bound, this equation corrects for the amount of KF·14/20mer·PP_i present.

The results are comparable: the first dGTP is incorporated at a rate of 50 s^{-1} and additional nucleotides are incorporated at a rate of 15 s^{-1} (data not shown).

Equilibrium Measurements. Experiments were done to ascertain the overall equilibrium constant for the conversion of bound 13/20mer and dATP to bound 14/20mer and PP_i catalyzed by KF. A 4-fold excess of KF over DNA was mixed with 5′-end-labeled 13/20mer, dATP, and varying levels of PP_i. The reaction was quenched with acid at 1-s time intervals up to 9 s. In all cases, the level of nucleotide incorporation did not change after 2 s, indicating a state of equilibrium had been attained. As shown in Table I, an average equilibrium constant of 2762 ± 919 was obtained.

As a result of the excess enzyme over DNA, the equilibrium constant measured in this experiment is for the enzyme–

DNA-bound species. Since all measurements made with the 13/20mer usually incorporate only a single nucleotide, only the equilibrium constant for this single incorporation event was obtained. Further, using conditions of excess enzyme over DNA results in the reaction reaching equilibrium relatively quickly and thereby avoiding the competing exonuclease reactions as well as the possible degradation of the 13/20mer by continued pyrophosphorolysis.

Derivation of Kinetic Rate Constants. The mathematical derivation of two unknown rate constants, the reverse rates for both the first and second conformational change steps, were obtained by combining the measurements of the pyrophosphorolysis reaction and of the overall equilibrium constant. On the basis of the results of the processive synthesis experiments, it was prudent to treat k_{pyro} as a net rate constant indicative of the flux of PP_i to labeled dATP as depicted in Scheme IV. Through the method of net rate constants (Cleland, 1975), k_{pyro} was expressed in terms of the individual rate constants of Scheme IV as shown in eq 1. The reverse rate of the first conformational change step (k_{-3}) is treated as irreversible under the given set of experimental conditions since the rate of labeled dNTP dissociation ($\sim$500 s^{-1}, based on a k_{on} for dNTP of 1×10^8 M^{-1} s^{-1}) from the KF·13/20mer·[^{32}P]dATP complex greatly exceeds its return. Furthermore, at saturating PP_i concentrations, the contribution of the PP_i binding step can be neglected. Finally, we assumed, for reasons to be discussed in the following section, that $k_c \gg k_{-3}$ and k_{-5}. These simplifications allow evaluation of k_{pyro} in terms of k_{-5} and k_{-3} as shown in eq 2.

Scheme IV

$$KF\cdot 14/20\cdot PP_i \underset{15\ s^{-1}}{\overset{k_{-5}}{\rightleftharpoons}} KF'\cdot 14/20\cdot PP_i \underset{4k_c}{\overset{k_c}{\rightleftharpoons}} KF'\cdot 13/20\cdot dATP \xrightarrow{k_{-3}} KF\cdot 13/20\cdot dATP$$

$$k_{pyro} = 0.31\ s^{-1} = \frac{1}{\frac{1}{k_{-3}} + \frac{4k_c + k_{-3}}{k_c k_{-3}} + \frac{15 + (k_c k_{-3}/(4k_c + k_{-3}))}{k_c k_{-5} k_{-3}/(4k_c + k_{-3})}} \quad (1)$$

For $k_c \gg k_{-3}$

$$k_{pyro} = \frac{1}{\frac{5}{k_{-3}} + \frac{60 + k_{-3}}{k_{-5}k_{-3}}} \quad (2)$$

To obtain a unique solution of k_{-5} and k_{-3}, the measured equilibrium constant of 2762 ± 919 was used as shown in eq 3. The rate and equilibrium constants, $K_{D,dNTP} = 5$ μM and $k_3 = 50$ s^{-1}, were measured previously (Kuchta et al., 1987). Taken together with those described here, $K_4 = 4$, $k_5 = 15$ s^{-1}, and $K_{D,PPi} = 230$ μM, eq 3 simplifies to eq 4. From eqs 2 and 4, $k_{-3} = 3$ s^{-1} and $k_{-5} = 15$ s^{-1}.

$$K_{EQ,DNA\text{-}bound} = \frac{1}{K_{D,dNTP}} \frac{k_3}{k_{-3}} K_4 \frac{k_5}{k_{-5}} K_{D,PPi} = 2762 \quad (3)$$

$$k_{-3}k_{-5} = 50 \quad (4)$$

Discussion

The kinetic mechanism for the correct incorporation of a dNTP into a DNA duplex has been described in some detail (Kuchta et al., 1987). A salient feature of this mechanism is the conformational change of a ternary KF·DNA·dNTP complex to a reactive form that, along with the dissociation of the product DNA_{n+1}, limits turnover of the polymerase. The mechanism for incorrect dNTP incorporation has an additional step that involves a conformational change of the ternary KF·DNA_{n+1}·PP_i product species that is also partially rate-limiting in misincorporation by the enzyme (Kuchta et al., 1988; Eger et al., 1991). While the physical nature of this step is unknown, it plays an important part in increasing the time of exposure of the 3′-terminus mismatch to exonuclease action. The results from the pulse–chase, pyrophosphorolysis, and pyrophosphate-exchange experiments described in this paper provide evidence for the existence of this second conformational change in correct nucleotide incorporation and, together with the measurements of equilibrium and rates of processivity, allow for its evaluation. In addition, the results provide accurate measures of the internal (enzyme-bound states) and external equilibrium for the polymerization process. Therefore, the mechanism in Scheme V, together with the associated rates in Table II, describes the complete kinetic pathway for correct nucleotide incorporation into a DNA primer strand catalyzed by KF.

Scheme V

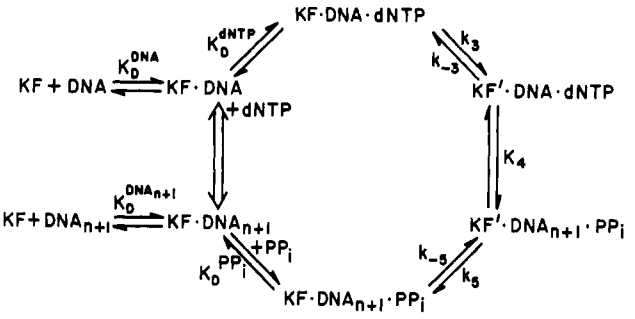

Table II: Rate and Equilibrium Constants for the Kinetic Mechanism of KF (Correct Incorporation)[a,b]

KF + 13/20mer ⇌ KF·13/20mer	K_D^{DNA} = 5 nM[c]
KF·13/20mer + dATP ⇌ KF·13/20mer·dATP	K_D^{dNTP} = 5 μM[c]
KF·13/20mer·dATP ⇌ KF′·13/20mer·dATP	k_3 = 50 s^{-1}[c]
	k_{-3} = 3 s^{-1}
KF′·13/20mer·dATP ⇌ KF′·14/20mer·PP_i	K_4 = 4
KF′·14/20mer·PP_i ⇌ KF·14/20mer·PP_i	k_5 = 15 s^{-1}
	k_{-5} = 15 s^{-1}
KF·14/20mer·PP_i ⇌ KF·14/20mer + PP_i	$K_D^{PP_i}$ = 230 μM
KF·14/20mer ⇌ KF + 14/20mer	K_D^{DNA} = 5 nM[c]

[a] Rate constants correspond to each step in Scheme V. [b] Based on the statistical deviation in the described experiments, these rate and equilibrium constants have an associated error of approximately ±5%. [c] Rate and equilibrium constants taken from Kuchta et al. (1987).

Pulse–chase experiments, first used to investigate the mechanism of yeast hexokinase (Rose et al., 1974; Wilkinson & Rose, 1979; Rose, 1980) and later with fructose bisphosphatase (Caperelli et al., 1978; Rahil et al., 1982), involve first "pulsing" the reaction with labeled substrate, allowing a pool of enzyme-bound intermediates to form, and then capturing this pool by "chasing" the reaction with a large excess of unlabeled substrate. The amount of product obtained in this experiment is then compared to that generated in a control reaction that is directly quenched with acid rather than "chased". Under pulse–quench conditions, the amount of product DNA formed after one enzyme turnover is equivalent to 80% of the enzyme concentration, while when "chased" the reaction produces an amount of the 14/20mer equivalent to that of the enzyme.

The pulse–chase results indicate that 20% of the E·DNA complex exists in a form suitable for nucleotide incorporation. Three possibilities exist: KF·13/20mer, KF·13/20 mer·[^{32}P]dATP, and KF′·13/20mer·[^{32}P]dATP. If 20% of the

enzyme is present as KF·13/20mer, then under chase conditions this binary complex would bind unlabeled dATP and be removed from observation. This would result in identical pulse–chase and pulse–quench curves. It is possible that the ternary complex KF·13/20mer·[^{32}P]dATP is the species of interest if the rate of dNTP dissociation is comparable to the forward rate for the first conformational change (k_3 in Scheme V). The 20% difference in the burst amplitudes of the two experiments would then be indicative of its partitioning between formation of product and release of dNTP. In order for the KF·13/20mer·[^{32}P]dATP to be chased through and to account for the 20% increase in radiolabeled product, computer simulations of Scheme V indicate that the dissociation rate of dATP from this complex must be ≤ 5 s^{-1}. Moreover, in the first 100 ms of the reaction (the pre-steady-state region), there would be a pronounced divergence between the pulse–quench and pulse–chase time courses for 14/20mer formation (data not shown). This arises since conversion of KF·13/20mer·[^{32}P]dATP to product is limited by k_3 (Scheme V) so that much of the 20% additional product would form in the pre-steady-state region of the time course. Finally, direct relaxation measurements of dATP binding to the binary KF·13/20mer complex are in accord with an off-rate constant for dATP ≥ 250 s^{-1} (Eger et al., 1991) consistent with earlier observations (Bryant et al., 1983). Thus, we conclude that KF·13/20mer·[^{32}P]dATP is not being significantly chased to products.

The ternary complex, KF′·13/20mer·[^{32}P]dATP, must transiently accumulate during the first enzyme turnover for three reasons. First, in Scheme V, k_{-3} is much slower than the chemical formation of product and, therefore, this substrate-bound species is insulated from decaying back to KF·13/20mer and [α-^{32}P]dATP under pulse–chase conditions, permitting its detection. Second, the time between chase with unlabeled substrate and the final quench of the reaction is approximately 50 ms as described under Results. With use of a minimal rate for k_4 (Scheme V) set at 150 s^{-1}, the time needed for the conversion of KF′·13/20mer·[^{32}P]dATP to KF′·[^{32}P]14/20mer·PP$_i$ is 5 ms (Jencks, 1987).[3] Therefore, the 50-ms period between introduction of the chase solution and the addition of the quench is more than adequate to observe its conversion to product. Third, confirmatory results are obtained through computer simulation of the data. From the mechanism in Scheme V, an accurate representation of the pulse–quench data was generated by plotting the predicted amount of the 14/20mer formed, both free and bound, versus time, whereas the pulse–chase data were accurately predicted when the amount of KF′·13/20mer·[^{32}P]dATP was also included.

The pulse–chase and quench comparison experiments thus indicate that 20% of the pool of the enzyme is in the KF′·13/20mer·dATP form. In order for this species to accumulate, it is necessary that a step after the chemical formation of the phosphodiester bond serves as a kinetic "roadblock".[4] If PP$_i$ were to dissociate from the ternary complex immediately after chemistry, in a step that would be both rapid and effectively irreversible, the KF′·13/20mer·dATP species would never transiently build up to any significant degree. An additional step, therefore, must be incorporated into the mechanism previously proposed for KF (Kuchta et al., 1987). Since 20% of the total amount of enzyme exists as KF′·13/20mer·dATP within the first turnover of the reaction, this additional step results in the KF′·14/20mer·PP$_i$ complex comprising the remaining 80% (shown below). Thus, the internal equilibrium constant is four ($K_{EQ} = 4$).

Scheme VI

Model A: $k_{ex} = k_{pyro}$

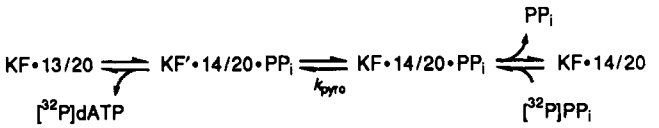

Model B: $k_{ex} > k_{pyro}$

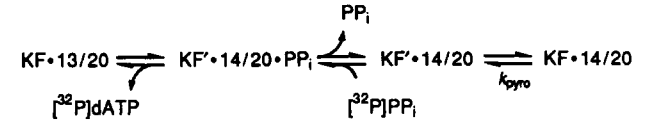

Pyrophosphorolysis, under conditions where the concentration of KF exceeds that of the 14/20mer (Figure 3), is described by a single first-order exponential. This is in contrast to a previous investigation (Kuchta et al., 1987) where biphasic kinetics (two exponentials) were observed. These earlier conclusions were found to be in error since the burst was irreproducible, owing to the methods by which the reaction was monitored in those experiments. In the present case, both the direct formation of dNTP and the amount of remaining 14/20mer were quantitated to assure a constant inventory. In the previous study, only the loss of label from the DNA primer strand was monitored so that unsuspected specific activity differences between the control and the reaction time points were not detected.

The observation that pyrophosphorolysis follows first-order kinetics is indicative of a rate-limiting step that occurs prior to or during chemical cleavage. Previous investigations have demonstrated an elemental effect on pyrophosphorolysis of 18–43 under k_{cat}/K_M conditions (Mizrahi et al., 1985; Kuchta et al., 1987), which suggests that the chemical step might be rate-limiting. However, experiments were done to ascertain the dissociation constant for [3′-^{35}S]14/20mer and [3′-^{32}P]-14/20mer bound to KF in a configuration such that pyrophosphorolysis would occur. Dissociation constants of 180 nM and 5 nM were obtained, respectively, indicating an elemental effect of 36 on the binding of DNA confirming our earlier conclusion that the absence of an elemental effect on polymerization but its appearance in the reverse direction required a higher ground-state free energy for the KF·[3′-^{35}S]14/20mer complex (Mizrahi et al., 1985). It is likely that there is little, if any, elemental effect on pyrophosphorolysis per se so that the first-order kinetics observed for the pyrophosphorolysis

[3] Computer modeling of the kinetic mechanism for KF has set a lower limit for the forward rate constant of the chemical step at 150 s^{-1}. Using values significantly lower than this results in a slower pre-steady-state burst rate as well as a lower burst amplitude for a correct nucleotide incorporation assay. Therefore, the reverse rate would then be 37.5 s^{-1} on the basis of the experimentally determined internal equilibrium constant. The time required for KF′·DNA·dNTP to traverse this chemical step (5 ms) was then determined by use of the equation

$$\tau = 1/k_{obs} = 1/(k_f + k_r)$$

In addition, the time for KF·DNA·dNTP to form KF′·DNA$_{n+1}$·PP$_i$ was determined to be approximately 53 ms, by use of a similar equation. This further confirms that the KF·DNA·dNTP species is not "chased" through to product since it would be partially quenched before conversion to product.

[4] As noted above, the accumulation of KF′·13/20mer·dATP also requires a kinetic "roadblock" preventing its rapid dissociation to free substrates, in accord with the conclusions deduced earlier by Kuchta et al. (1987, 1988) from comparison of thioelemental effects observed for correct and incorrect incorporation of dNTP.

reaction is indicative of a rate-limiting step prior to cleavage of the phosphodiester bond, in accord with the conclusions drawn from the pulse–chase experiments.

There are two kinetic sequences in accord with the results of the pyrophosphorolysis experiment that differ only in the placement of the slow nonchemical step relative to PP_i release and chemical catalysis. The two possible sequences and the predicted results for each are presented in Scheme VI. Although model A is suggested by the pulse–chase experiments, confirmatory evidence was sought through measurement of the rate of pyrophosphate exchange. This experiment monitors the exchange of a radiolabel from PP_i into the dATP substrate under conditions of alternating polymerase/pyrophosphorolysis activities. For both models, the rate measured in the pyrophosphorolysis experiments is that for the formation of [^{32}P]dATP from the KF·14/20mer ground state. The rate of pyrophosphate exchange, designated k_{ex}, measures [^{32}P]dATP formation from the [^{32}P]PP_i-binding step, and therefore may be greater than or equal to that measured in the pyrophosphorolysis experiments.

In model A, the KF·14/20mer complex must undergo a slow conformational change (designated k_{pyro}) prior to exchange of PP_i, while in model B, PP_i can bind a different conformation of the KF·14/20mer complex and thus bypass this slow step. The expected result for model B is a faster rate of turnover than in the pyrophosphorolysis experiments described previously. The results obtained show a rate constant of pyrophosphate exchange that is almost identical with the rate constant for pyrophosphorolysis (0.17 s^{-1} and 0.31 s^{-1}, respectively). Thus, it can be concluded that the conformational change of the KF′·14/20mer·PP_i species occurs after phosphodiester bond formation but prior to the release of PP_i as depicted in Scheme V and model A of Scheme VI.

Having firmly established the existence and location of the conformational change step of the KF′·14/20mer·PP_i complex on the kinetic pathway for KF, we evaluated its rate. On the basis of the results of the previous experiments we concluded that the forward rate for this conformational change step was slow relative to the rate at which chemical bond formation took place. This rate might, therefore, be comparable in magnitude to the rate of the first conformational change (50 s^{-1}). Product formation occurs prior to the second conformational change step; thus, the rate for incorporation of a single correct nucleotide will depend only on the rate of the first conformational change step. The effect of these two forward rates on the net flux of the reaction would only be observed when multiple nucleotides are incorporated; therefore, the rates at which KF processively synthesized the 17/20mer, 16/20mer, 15/20mer, and 14/20mer from the 13/20mer were measured. Computer simulations verified that the predicted data curves were relatively insensitive to the reverse rates of the two conformational change steps due to the favorable equilibrium toward product and set a value of 15 s^{-1} for the forward rate constant of the second conformational change step.

Evaluation of the overall equilibrium constant for the polymerization reaction was necessary to obtain unique values for the reverse rates of the two conformational change steps (k_{-3} and k_{-5} in Scheme V). Equilibrium constants in the presence of pol I (McClure & Jovin, 1975) and KF (Kuchta et al., 1987) have been determined previously; however, the experimental design used to obtain these values may have introduced a further complication. Both used catalytic amounts of enzyme and measured the equilibrium reached after multiple turnovers. As noted in the pyrophosphorolysis experiments described above, a significant amount of exonuclease activity was observed over the course of 20 s (data not shown). While both investigations took this into account by including a replacement pool of the nucleotide that would be hydrolytically cleaved from the 3′-terminus by exonucleolytic degradation, the possibility remains that the equilibrium measured is compromised by action of the combined polymerase/exonuclease activities. To avoid this complication and to measure the equilibrium constant for bound substrates, conditions were chosen where all the DNA was enzyme-bound and the reaction was constrained to a 9-s time interval. As a result, the equilibrium distribution of bound substrates and products ($K_{EQ,bound}$ = 2762 ± 919) is obtained in approximately 2 s, a time not sufficient for an appreciable amount of exonuclease activity to occur.

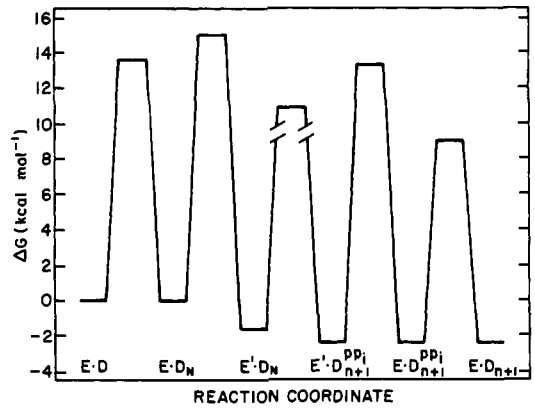

FIGURE 5: Gibbs free energy profile for correct nucleotide incorporation at a standard state of 5 μM dNTP and 230 μM PP_i. The on rates for dNTP and PP_i are assumed to be limited by diffusion. The forward rate for the chemical step for correct incorporation was set at 4000 s^{-1} and the reverse rate at 1000 s^{-1} on the basis of the assumption that the chemical step is fast compared to all other steps.

These experiments collectively permit the direct evaluation of the minimal kinetic pathway for the polymerization reaction of KF. The results of the pulse–chase experiments established the existence of a second conformational change step and characterized the internal (chemical) equilibrium constant. Pyrophosphate-exchange experiments confirmed that this second conformational change step occurred after chemical bond formation but prior to release of PP_i. Measurements of the rates of processive synthesis and pyrophosphorolysis together with the determination of the overall equilibrium constant permitted evaluation of both the forward and reverse rates for this nonchemical step as well as the dissociation constant of PP_i from the KF·DNA complex. Values of rate and equilibrium constants associated with Scheme V are listed in Table II and graphed as a free energy profile in Figure 5. It is clear that the first nonchemical step limits the rate of a single nucleotide incorporation while the second limits the rate of processive synthesis. The two are separated by chemical bond formation that is fast and favors product formation by a factor of 4.

The structural changes and function of the two nonchemical steps that occur before and after phosphodiester bond formation are unknown. Results obtained through NMR investigations of KF with bound substrates suggest that the first conformational change might involve the reorientation of the terminal phosphate groups of the dNTP from a state with a magnesium counterion to one where this group is bound to the peptide side chain through ionic interactions (Ferrin & Mildvan, 1986). An alternate hypothesis, based on the incorporation of methylated dATP residues into a homopolymer by KF, postulates that this conformational change involves "tightening" of the dNTP into the active site as a result of

hydrogen bonding to the template base, analogous to a two-step binding mechanism (Engel & von Hippel, 1978). If hydrogen bonding of the incoming nucleotide to the template base were to occur in the first conformational change step, then the chemical step should exhibit a significant amount of error discrimination. This is based on the observation that nucleotides that form nonstandard Watson–Crick base pairs show unequal angles between the glycosidic bond and the plane perpendicular to the purine/pyrimidine ring system for each base (Kennard, 1985). The effect would be a perturbation in the geometrical alignment of the 3′-hydroxyl moiety of the primer strand relative to the α-phosphate group of the incoming nucleotide and a concomitant decrease in the rate of chemical bond formation. A reduction in the rate of chemical catalysis for a misincorporation event has been observed (Kuchta et al., 1988) as well as an associated effect on fidelity.

The physical nature of the conformational change of the $KF'{\cdot}DNA_{n+1}{\cdot}PP_i$ species to form the $KF{\cdot}DNA_{n+1}{\cdot}PP_i$ complex is likewise unknown. Based on the symmetry of the kinetic mechanism a two-step release mechanism for PP_i parallels the two-step binding mechanism for dNTP. However, unlike dNTP, PP_i is less likely to bind in an incorrect conformation. An alternative hypothesis is that this second conformational change represents the movement of the primer strand to the exonuclease site and subsequent hydrolysis if the nucleotide has been misincorporated. A further, intriguing hypothesis is that this second conformational change step represents translocation of the enzyme along the DNA duplex to a site where an additional nucleotide may be incorporated, which would occur at each polymerization cycle. The basis for this suggestion is the observation that, under single turnover polymerization conditions, PP_i has been shown to be a competitive inhibitor of dNTP, thus suggesting that PP_i and dNTP bind the same enzyme–DNA complex (unpublished data). For this to occur, the enzyme must undergo translocation prior to PP_i release. Further, the fact that this conformational change step is isoenergetic is in accord with von Hippel's hypotheses and observations of protein translocation on nucleic acids (Berg et al., 1981; Winter & von Hippel, 1981), although the rate constant is far less than simple two-dimensional diffusion by a protein along a DNA strand. Experiments to determine the physical nature of this second conformational change step and to ascertain its relationship to the degree of processivity of different polymerases are in progress.

References

Anderson, K. S., Sikorski, J. A., & Johnson, K. A. (1988) *Biochemistry 27*, 7395–7406.

Bambara, R. A., Uyemura, D., & Lehman, I. R. (1976) *J. Biol. Chem. 251*, 4090–4094.

Barshop, B. A., Wrenn, R. F., & Frieden, C. (1983) *Anal. Biochem. 130*, 134–145.

Berg, O. G., Winter, R. B., & von Hippel, P. H. (1981) *Biochemistry 20*, 6929–6948.

Brody, R. S., & Frey, P. A. (1981) *Biochemistry 20*, 1245–1252.

Bryant, F. R., Johnson, K. A., & Benkovic, S. J. (1983) *Biochemistry 22*, 3537–3546.

Burgers, P. M. J., & Eckstein, F. (1979) *J. Biol. Chem. 254*, 6889–6893.

Caperelli, C. A., Frey, W. A., & Benkovic, S. J. (1978) *Biochemistry 17*, 1699–1704.

Carroll, S. S., & Benkovic, S. J. (1990) *Chem. Rev. 90*, 1291–1307.

Cleland, W. W. (1975) *Biochemistry 14*, 3220–3224.

Eger, B. T., Kuchta, R. D., Carroll, S. S., Benkovic, P. A., Dahlberg, M. E., Joyce, C. M., & Benkovic, S. J. (1991) *Biochemistry 30*, 1441–1448.

Engel, J. D., & von Hippel, P. H. (1978) *J. Biol. Chem. 253*, 935–939.

Englisch, V., Gauss, D., Freist, W., Englisch, S., Sternbach, H., & von der Haar, F. (1985) *Angew. Chem., Int. Ed. Engl. 24*, 1015–1025.

Ferrin, L. J., & Mildvan, A. S. (1986) *Biochemistry 25*, 5131–5145.

Freemont, P. S., Friedman, J. M., Beese, L. S., Sanderson, M. R., & Steitz, T. A. (1988) *Proc. Natl. Acad. Sci. U.S.A. 85*, 8924–8928.

Gupta, A. F., & Benkovic, S. J. (1984) *Biochemistry 23*, 5874–5881.

Jencks, W. P. (1987) *Catalysis in Chemistry and Enzymology*, pp 586–589, Dover Publications, New York.

Johnson, K. A. (1986) *Methods Enzymol. 134*, 677–705.

Joyce, C. M., & Grindley, N. D. F. (1983) *Proc. Natl. Acad. Sci. U.S.A. 80*, 1830–1834.

Kennard, O. (1985) *J. Biomol. Struct. Dyn. 3*, 205–226.

Kornberg, A. (1980) *DNA Replication*, Freeman, San Francisco.

Kuchta, R. D., Mizrahi, V., Benkovic, P. A., Johnson, K. A., & Benkovic, S. J. (1987) *Biochemistry 26*, 8410–8417.

Kuchta, R. D., Benkovic, P. A., & Benkovic, S. J. (1988) *Biochemistry 27*, 6716–6725.

Lanzetta, P. A., Vlvarez, L. J., Reinach, P. S., & Candia, O. A. (1979) *Anal. Biochem. 100*, 95–97.

Maniatis, T., Fritsch, E. I., & Sambrook, J. (1982) *Molecular Cloning. A Laboratory Manual*, Cold Spring Harbor Laboratory, Cold Spring Harbor, NY.

McClure, W. R., & Jovin, T. M. (1975) *J. Biol. Chem. 250*, 4073–4080.

Mizrahi, V., Henrie, R. N., Marlier, J. F., Johnson, K. A., & Benkovic, S. J. (1985) *Biochemistry 24*, 4010–4018.

Mizrahi, V., Benkovic, P. A., & Benkovic, S. J. (1986a) *Proc. Natl. Acad. Sci. U.S.A. 83*, 231–235.

Mizrahi, V., Benkovic, P. A., & Benkovic, S. J. (1986b) *Proc. Natl. Acad. Sci. U.S.A. 83*, 5769–5773.

Ollis, D. L., Brick, P., Hamlin, R., Xuong, N. G., & Steitz, T. A. (1985) *Nature (London) 313*, 762–766.

Patel, S. S., Wong, I., & Johnson, K. A. (1991) *Biochemistry 30*, 511–525.

Rahil, J. F., de Maine, M. M., & Benkovic, S. J. (1982) *Biochemistry 21*, 3358–3363.

Rose, I. A. (1980) *Methods Enzymol. 64*, 47–59.

Rose, I. A., O'Connell, E. L., Litwin, S., & Bar Tana, J. (1974) *J. Biol. Chem. 249*, 5163–5168.

Setlow, P., Brutlag, D., & Kornberg, A. (1972) *J. Biol. Chem. 247*, 224–231.

Wilkinson, K. D., & Rose, I. A. (1979) *J. Biol. Chem. 254*, 12567–12572.

Winter, R. B., & von Hippel, P. H. (1981) *Biochemistry 20*, 6948–6960.